RAPID COMMUNICATIONS

PHYSICAL REVIEW A VOLUME 42, NUMBER 9 1 NOVEMBER 1990

# Energy analysis of time-dependent wave functions: Application to above-threshold ionization

K. J. Schafer and K. C. Kulander
*Physics Department, Lawrence Livermore National Laboratory, Livermore, California 94550*
(Received 20 February 1990)

We present a method for calculating energy-resolved properties from time-dependent wave functions. As a first application of the method we calculate above-threshold ionization (ATI) spectra and energy-resolved angular distributions from hydrogen ionized by an intense, short-pulse laser at 532 nm. Below saturation the ATI peaks decrease according to an (intensity-dependent) power law. At the onset of saturation a plateau forms in the spectrum, reminiscent of plateaus seen experimentally in harmonic spectra observed during multiphoton ionization.

## I. INTRODUCTION

We present a method for extracting energy-resolved information from a time-dependent (TD) wave function that has been calculated on a grid. TD studies of dynamical phenomena in quantum mechanics have become ubiquitous in physics and chemistry. Typical applications, which include atomic collisions, scattering from surfaces, reactive scattering, and multiphoton ionization, require the solution of either the time-dependent Schrödinger equation (TDSE) or a set of TD self-consistent-field equations by evolving an initial state forward in time under the action of a TD Hamiltonian. Experimentally measurable quantities are then calculated from the wave function in the asymptotic region.

The motivation for solving these equations on a numerical grid derives in the main from two sources: (i) A grid allows great flexibility in describing systems that undergo rearrangement and/or bound-to-continuum transitions and (ii) there exist a number of very fast time-evolution schemes based on discretized Hamiltonians, the choice of discretization being based upon the physics of the particular problem under consideration.

The efficient extraction of energy-resolved information is not, however, straightforward given a grid-calculated wave function. Projection of the TD wave function onto states of definite energy requires either the calculation of these states (as eigenstates of the asymptotic Hamiltonian) or their approximation by an analytic form. In the general case neither of these alternatives is attractive since the computation and storage of eigenstates is prohibitive in multiple dimensions and analytic approximations fail if the energy region of interest is close to a threshold, or if the wave function has not yet reached a region where asymptotic states can be used. In the next section we present a method for extracting energy-resolved quantities via a window operator that circumvents these difficulties. The method is powerful and very flexible, its resolution and accuracy being separately specifiable. Following that, we present results from our first use of the method: an exact calculation of the above-threshold (ATI) spectrum of hydrogen at 532 nm. These results are quite striking in their own right and could not have been easily obtained without the energy analysis that we outline below.

## II. METHOD

We assume the general case in which a TD calculation has resulted in a final-state wave function $\psi_f$. Labeling the discretized asymptotic Hamiltonian as $\hat{H}_0$, we concentrate for the moment on calculating $P_\gamma(E_k)$ the total probability of finding a particle in a final-state "energy bin" of width $2\gamma$ (where $\gamma$ is not infinitesimal) centered about $E_k$. We do this by defining a window operator,

$$\hat{W}(E_k,n,\gamma)\equiv\gamma^{2n}/[(\hat{H}_0-E_k)^{2n}+\gamma^{2n}]\,, \tag{1}$$

which projects onto all eigenstates $|m\rangle$, bound and continuum, of $\hat{H}_0$ in the range $E_k\pm\gamma$. The matrix elements of $\hat{W}$ yield an approximation for $P_\gamma(E_k)$:

$$P_\gamma(E_k)\approx\langle\psi_f|\hat{W}|\psi_f\rangle = \sum_{|m\rangle}|\langle\psi_f|m\rangle|^2\left(\frac{\gamma^{2n}}{(E_m-E_k)^{2n}+\gamma^{2n}}\right). \tag{2}$$

As $n$ is increased the shape of the window function in the large parentheses in Eq. (2) rapidly becomes rectangular with very little overlap between adjacent energy bins. Note also that as $n$ is increased the bin width remains constant at $2\gamma$. A complete spectrum with a resolution of $\approx 2\gamma$ is built up by calculating $P_\gamma(E_k)$ for a set of $E_k$ where $E_{k+1}=E_k+2\gamma$.

The integrated probability over an energy range $E\pm\Delta E$, $\Delta E\gg\gamma$, can be accurately approximated by summing the calculated values of $P_\gamma(E_k)$ that fall within the energy range. This is useful for determining, for example, the total probability contained in a particular continuum resonance. As the bins become more rectangular, the sum becomes independent of $\gamma$, meaning that integrated quantities can be calculated with relatively large energy bins. We find that this property holds quite well already at $n=2$.

The shape and location of a particular resonance structure in the spectrum can be found by choosing $\gamma$ to be smaller than the width of the resonance. Although it might seem from Eq. (2) that the resolution of our window function is limited by the (energy-dependent) spacing between the eigenstates of $\hat{H}_0$, which is dictated by the overall size of the computational grid used in calculating

 

$\psi_f$, arbitrarily fine resolution can be achieved by performing the analysis on an expanded grid using $\psi_f$ from the smaller grid. When dealing with bound states, $\hat{W}$ plays the role of a line-broadening function, familiar from spectral methods using time-dependent correlation functions. When $\gamma$ is chosen to be smaller than the separation between bound states, the location and population of a particular bound state can be found by fitting to the right-hand side of Eq. (2) those values of $P_\gamma(E_k)$ that fall close to the bound-state energy.

As important as its flexibility is the ease with which we can evaluate the matrix elements of $\hat{W}$. We first note that solving the system

$$[(\hat{H}_0 - E_k)^{2^{n-1}} + i\gamma^{2^{n-1}}]|\chi_k\rangle = |\psi_f\rangle \quad (3)$$

yields $P_\gamma(E_k)$ as $\gamma^{2^n}\langle\chi_k|\chi_k\rangle$. In this form iterative solution methods such as conjugate gradient can be efficiently applied. The vector $|\chi_k\rangle$ provides an excellent initial guess for finding $|\chi_{k+1}\rangle$. It is also always possible to factor Eq. (3) into terms involving only single powers of $\hat{H}_0$. For $n=2$, for example, we can write

$$(\hat{H}_0 - E_k + \sqrt{i}\gamma)(\hat{H}_0 - E_k - \sqrt{i}\gamma)|\chi_k\rangle = |\psi_f\rangle . \quad (4)$$

This form is particularly suitable when $\hat{H}_0$ is either exactly or approximately separable. With any of these methods the work to calculate $P_\gamma(E_k)$ for a fixed energy range scales as $2^n/\gamma$.

To calculate energy-resolved features of $\psi_f$ we can apply the window operator to the wave function itself as $\phi_k = \hat{W}\psi_f$. Forming the product $\phi_k^* \phi_k$, integrating over irrelevant coordinates and summing over several adjacent energy bins, we obtain, for example, angular distributions for photoelectrons in a narrow energy range.

## III. APPLICATION

Recent experimental interest in the photoelectron spectrum from atoms in very intense, pulsed laser fields[1] has encouraged the use of TD simulations for their study. This is a regime where the laser-atom interaction is no longer a perturbation of the field-free atomic states.[2,3] We have integrated the TDSE for a hydrogen atom interacting with linearly polarized 532-nm photons (2.33 eV). We studied a range of intensities $I$ from $10^{13}$ to $10^{14}$ W/cm$^2$ using a fourteen optical cycle trapezoidal pulse with two cycle linear ramps (ten constant cycles). This gives a bandwidth that is small compared to the laser frequency and has low sideband noise.

The time integration was carried out using a spherical coordinate finite difference code that employs an angular momentum decomposition of the wave function. Each angular momentum channel is expanded on a radial grid and the resulting coupled equations are solved using a Peaceman-Rachford propagator.[3] In order to contain the ionized wave function, the grid included radial points up to 2000 a.u. and partial waves up to $l=150$ for the highest intensities. Our results have been checked for convergence with respect to the integration parameters.

Figure 1 is a logarithmic plot of $P_\gamma(E_k)$ generated using $n=2$, $2\gamma=0.025$ eV for $I=2\times10^{13}$ W/cm$^2$. The analysis

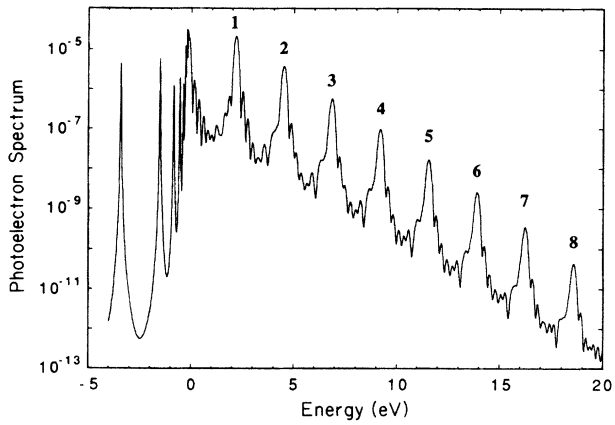


FIG. 1. Photoelectron spectra $P_\gamma(E_k)$ for 532 nm, $I=2\times10^{13}$ W/cm$^2$, $n=2$, $2\gamma=0.025$ eV.

was performed after the complete fourteen cycle pulse. This spectrum is typical of our results. The population remaining in Rydberg levels, which we observed to varying degrees at every intensity, is evident below the ionization threshold. The isolated bound eigenstates have a width which is proportional to $\gamma$. In the continuum there are a series of ATI peaks up to order $S=8$ (where $S=0$ denotes absorption of six photons, the minimum number necessary to exceed the field-free ionization threshold). $S=0$ is closed for intensities above $1.4\times10^{13}$ W/cm$^2$ due to the ponderomotive shift of the ionization limit but the $S=0$ peak is still visible in Fig. 1 as a population in the upper Rydberg levels. In contrast to the bound states, the continuum peaks have a width (i.e., the full width at half maximum) which is equal to the bandwidth of the laser pulse ($\approx 0.23$ eV). The sideband structure on each peak closely mimics the sideband structure of the trapezoidal laser pulse. The Rydberg-like substructure seen in short-pulse experiments[1] is not found because the linear ramps of our pulse are too rapid to produce significant excitation of these transient resonances. In an actual experiment the atoms in the focal volume of the laser experience a range of ponderomotive shifts.[4] To make a direct connection to our single atom calculation it is necessary to average over calculations at different intensities.

All of the peaks in Fig. 1 are 2 or more orders of magnitude above the background. This is remarkable in light of the fact that the $S=8$ peak corresponds to the ionization of less than one part in $10^9$ of the total wave function during the pulse. This sensitivity is far beyond that of current experimental technique. Information about higher-order ATI peaks may be contained in experimental data on high-order harmonic generation, if a strong connection between ATI and harmonic generation can be established.[5,6] The computer time necessary to analyze the wave function is a few minutes, in contrast to several hours to obtain $\psi_f$. At the end of the pulse the $l$ channels decouple and can be separately analyzed, with a consequent gain in speed. This approach can also be used for nonhydrogenic (even $l$-dependent) potentials with no additional complications. Previous calculations have shown that the use of such potentials can provide a good descrip-

tion of sequential ionization of rare-gas atoms, for which the most experimental data are available.[7]

Figure 2 is our main result. The partial ionization rate of all open ATI channels up to a maximum of $S=9$ are shown for $I=(1, 2, 4, 6, \text{ and } 10)\times10^{13}$ W/cm$^2$. These rates were calculated by summing $P_\gamma(E_k)$ over the energy bins under each peak and dividing by the length of the constant part of the pulse. The partial rates we quote are insensitive to the pulse length (i.e., adding more constant cycles to our pulse yields the same partial rates). Thus our rates correspond closely to what one would calculate in a standard time-independent approach. To our knowledge this is the first exact, complete ATI calculation to span such a wide range of nonperturbative intensities. At the lowest intensity, $1\times10^{13}$ W/cm$^2$, we can compare our calculated rates with modified (to account for the shift of the ionization limit) perturbation theory (PT) calculations[8] as well as to Floquet calculations (for the low-order rates) and find agreement to about 10%. Above $1\times10^{13}$ W/cm$^2$ the number of $l$'s needed to accurately integrate the TDSE rises very steeply, characteristic of the regime where PT breaks down. At higher intensities our rates fall progressively below the perturbative rates.[2,8]

The most striking feature of Fig. 2 is that, despite the fact that the laser-atom interaction is very strong, the higher-order rates display a near power-law dependence. This behavior holds well even at $6\times10^{13}$ W/cm$^2$ but breaks down by $1\times10^{14}$ W/cm$^2$. The four lowest data sets may be fit approximately with a simple PT-like form $R_N\approx A(\sigma I)^N$, where $R_N$ is the partial ionization rate for the channel corresponding to the absorption of $N$ photons. In PT, $A$ is a prefactor and $\sigma$ is proportional to a dipole transition strength, both being a constant independent of intensity. Our data would indicate a weak intensity dependence in $A$ and a slow decrease in $\sigma$ with increasing intensity. The simple power-law dependence is, however, broken for the lowest open channel in each case. The degree to which this lowest-order rate deviates from the behavior of the higher-order rates is directly proportional to the distance of the ATI peak from the ionization threshold. Thus the $S=0$ rate for $1\times10^{13}$ W/cm$^2$ falls below the trend set by $S=1$–5 and its location is only 0.1 eV above the ionization threshold. At $2\times10^{13}$ W/cm$^2$ the $S=1$ rate is in good agreement with the trend of the higher-order rates and the ATI peak is located 2.2 eV above threshold. The same pattern is repeated as the $S=1$ channel closing is approached in the (4 and 6)$\times10^{13}$ W/cm$^2$ runs.

At the highest intensity, $1\times10^{14}$ W/cm$^2$, over 1% of the electron probability is reaching the continuum during each optical cycle, signaling the onset of saturation and the breakdown of any time-independent treatment. The first three or four ATI peaks at $1\times10^{14}$ W/cm$^2$ form a plateau that is quite distinct from the behavior at lower intensities. This plateau is reminiscent of plateaus seen in harmonic spectra from atoms undergoing multiphoton ionization.[5,6] Recently it has been proposed that the plateaus seen in harmonic spectra should have an analog in ATI spectra.[9]

We also calculated angular distributions for each of the ATI peaks using the prescription outlined at the end of the previous section. In Fig. 3 the distributions for the $S=1$, 2, and 3 peaks from Fig. 1 are plotted. These agree well with experimental results[10] that used an intensity of about $1.6\times10^{13}$ W/cm$^2$. The $S=1$ curve is also in excellent agreement with Floquet calculations[8] for this intensity. We find the angular distributions of the low-order ATI peaks narrow with increasing order or intensity but that this behavior breaks down for higher-order peaks and higher intensities. The distributions decrease in width initially as the order is increased, pass through a minimum, and then broaden at successively higher orders. This behavior has been observed in hydrogen.[10]

We note three features of our results which provide insight into the atom-laser interaction at high-field intensity. First, all ATI peaks were found to be at their ponderomotively shifted values until $1\times10^{14}$ W/cm$^2$. At this intensity the $S=1$ peak was overshifted by about 0.06 eV which placed the peak maximum below the ionization threshold. Second, although the low-order peak widths were always the same as the pulse bandwidth, at intensities higher than $2\times10^{13}$ W/cm$^2$ the higher-order peaks were significantly broadened. We checked that this was not an artifact of any of the integration parameters.

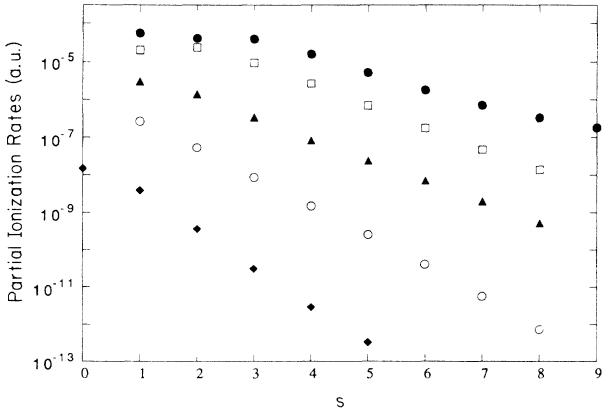


FIG. 2. Partial ionization rates in atomic units. The intensities are (♦) $1\times10^{13}$, (○) $2\times10^{13}$, (▲) $4\times10^{13}$, (□) $6\times10^{13}$, and (●) $1\times10^{14}$ W/cm$^2$.

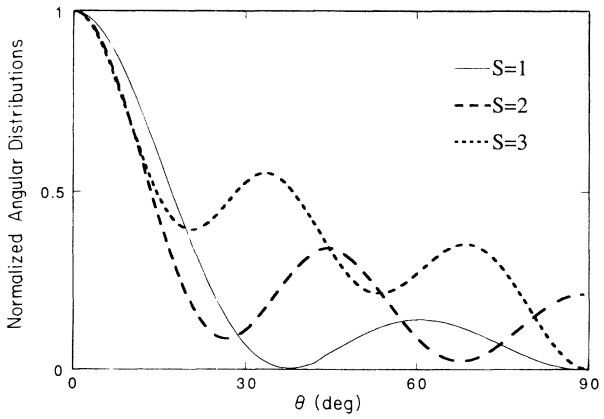


FIG. 3. Angular distributions for the $S=1$, 2, and 3 ATI peaks in Fig. 1.

Perhaps most interestingly, we found that at all intensities, regardless of the degree of dressing that the electron underwent during the laser pulse, during the turn-off phase of the pulse the $l$ distribution "collapsed" back down into the low partial waves. Thus, although we needed to use 150 $l$ channels to converge the calculation for $1\times10^{14}$ W/cm$^2$, $\psi_f$ contained no meaningful contribution from $l \geq 16$.

We have presented an alternative, powerful, and efficient method for extracting final-state distributions from TD wave functions which can be very useful in many areas of physics and chemistry. We applied this method to the very timely problem of the ATI of hydrogen and obtained the most detailed photoelectron spectra for a real atomic system ever calculated. The remarkable sensitivity of our analysis has revealed several novel features of the ATI spectra which were only briefly mentioned here. A more complete description which will include additional calculations at near-resonant intensities is planned to be the subject of a future publication.

## ACKNOWLEDGMENTS

This work was performed under auspices of the U.S. Department of Energy at Lawrence Livermore National Laboratory under Contract No. W-7405-ENG-48. Partial support was provided by National Science Foundation Grant No. PHY87-11139.

[1]R. R. Freeman *et al.*, Phys. Rev. Lett. **59**, 1092 (1987); M. D. Perry, A. Szöke, and K. C. Kulander, Phys. Rev. Lett. **63**, 1058 (1989); P. Agostini *et al.*, Phys. Rev. Lett. **63**, 2208 (1989); H. Rottke *et al.*, Phys. Rev. Lett. **64**, 404 (1990).

[2]S.-I. Chu and J. Cooper, Phys. Rev. A **32**, 2769 (1985).

[3]K. C. Kulander, Phys. Rev. A **35**, 445 (1987).

[4]T. J. McIlrath *et al.*, Phys. Rev. A **40**, 2770 (1989).

[5]M. Ferray, A. L'Huillier, X. F. Li, L. A. Lompre, G. Mainfrey, and C. Manus, J. Phys. B **21**, L31 (1988).

[6]K. C. Kulander and B. W. Shore, Phys. Rev. Lett. **62**, 524 (1989).

[7]K. C. Kulander, Phys. Rev. A **38**, 778 (1988).

[8]R. M. Potvliege and R. Shakeshaft, Phys. Rev. A **39**, 1545 (1989); **41**, 1609 (1990); M. Doerr and R. Shakeshaft (private communication).

[9]J. Javanainen, Q. Su, and J. H. Eberly, Phys. Rev. Lett. **62**, 881 (1989).

[10]B. Wolff, H. Rottke, D. Feldmann, and K. H. Welge, Z. Phys. D **10**, 35 (1988).